



Diffusion studies in polarized reverse osmosis processes by holographic interferometry

J. Fernández-Sempere*, F. Ruiz-Beviá, R. Salcedo-Díaz, P. García-Algado

Chemical Engineering Department, University of Alicante. Apartado 99, 03080 Alicante, Spain

Abstract

When a reverse osmosis process takes place, the build-up of a polarization layer occurs due to both convective and diffusive forces. Once the process ceases and no driving force is applied, this polarization layer disappears as a consequence of a diffusion process. This disappearance can be studied by means of holographic interferometry.

© 2008 Elsevier Ltd. All rights reserved.

Keywords: Diffusion; Holographic interferometry; Reverse osmosis; Disappearance; Polarization layer

1. Introduction

For many years, holographic interferometry (HI) is an optical method widely used to measure diffusion coefficients in liquids [1–4] and in transparent gels [5–7]. In addition, the technique can also be used to study more complex processes in which diffusion phenomena appear, as in reverse osmosis (RO).

RO is a separation process through membranes in which, applying pressure, the water of a saline solution is forced to pass through a semi-permeable membrane. It can be described as a process in which the transport of solvent and solutes through the membrane is basically controlled by the solution and diffusion mechanisms, in clear contrast with the ordinary filtration where the separation is based on the size of particles and pores of membranes. RO is able to separate particles of up to $0.0001\ \mu\text{m}$ of diameter (the size of the ions); that is the reason that its main application is the brackish water desalination for obtaining fresh water.

One of the main limitations of membrane processes is the build-up of the concentration polarization layer. The phenomenon consists of the accumulation of solute on the surface of the membrane as a consequence of the convective driving forces. These forces cause the movement of solute towards the membrane which, depending on the

retention capacity of the membrane, retains most of the solute and allows the solvent to pass with a certain amount of solute. Whereas other fouling membrane phenomena (precipitation of salts, adsorption of solutes and even formation of a gel layer in the case of the ultrafiltration) still continue after finishing the filtration process, the polarization concentration talks about solute in solution that is retained near the membrane in a non-permanent way. It is a reversible process, so that this polarization layer will disappear by diffusion when stopping the driving force. As a result of the formation of the concentration polarization layer, a decrease of the permeate volume, and therefore of the process yield, takes place.

The phenomenon is known as concentration polarization and it is easier to study its properties through measurements of the dissolved solute profiles in an unstirred batch cell than in cross-flow processes (Fig. 1). The reason being that in cross-flow processes the thickness of the boundary layer is limited by the flow parallel (especially if it is turbulent) to the membrane. In cross-flow, if steady state is reached, the convective solute flux to the membrane surface is balanced by the solute flux through the membrane plus the diffusive and convective flow back to the bulk of the feed. The concentration profile near the membrane is usually stable and the maximum concentration is not very high. However, in the case of membrane processes carried out in an unstirred batch cell or dead-end conditions, a steady state is not easily reached,

*Corresponding author. Tel.: +34 96 5903826; fax: +34 96 5903464.
E-mail address: julio.fernandez@ua.es (J. Fernández-Sempere).

Notation

C	concentration of the solute [ML^{-3}]
C_o	concentration of solute in the bulk solution [ML^{-3}]
C_m	maximum concentration of solute at the membrane surface [ML^{-3}]
C_p	concentration of solute in the permeate [ML^{-3}]
D	diffusion coefficient [LT^{-2}]
d	thickness of the liquid that the light passes through [L]
J_w	average volumetric permeate flux with pure water [LT^{-1}]
k	interference fringe order
n	refractive index
n_o	refractive index of the bulk solution

P	pressure [$\text{ML}^{-1}\text{T}^{-2}$]
R_m	membrane hydraulic resistance to the flux with pure water [$\text{ML}^{-3}\text{T}^{-1}$]
T	time [T]
y	space coordinate

Greek letters

δ	thickness of the boundary layer [L]
λ	wavelength [L]

Abbreviations

HI	holographic interferometry
RO	reverse osmosis

concentrations reached at the membrane surface (C_m) are very high and the thickness of the boundary layer (δ) grows continuously with time (Fig. 2).

A polarization layer builds-up as a consequence of the convective driving forces acting towards the membrane and the diffusive phenomenon from the membrane to the solution bulk. However, when the driving force (pressure) ceases (Fig. 3), convection disappears and only diffusion remains. The result is C_m decreases, δ grows and, consequently, the polarization layer disappears very slowly.

The experimental determination of the concentration profiles in the polarization layer during membrane processes is a problem still not completely solved. Several authors have studied the polarization layer, most of them measuring the concentration gradients by means of conductivity techniques [8–10]. These conductivity techniques are useful to study the polarization layer in RO, but concentration can only be measured at the points where the probes have been placed, and therefore it is not possible to completely visualize the polarization layer.

The use of non-destructive optical techniques permits a deep study of what happens near the membrane during these transport processes. Classic interferometry [11–16] and holographic interferometry [17–20] have been successfully used to measure concentration profiles near the membrane during mass transfer processes. The knowledge

of these profiles allows the evaluation of which are the mechanisms implied in the process.

The objective of this work is to use holographic interferometry to study the diffusion phenomenon that takes place once the pressure ceases in RO processes. The process has been studied using potassium nitrate solutions. The formation and the disappearance of the polarization layer and its evolution with time during the process of RO in a module by loads and without agitation can be visualized in real time by means of a holographic interferometric set-up.

Using holographic interferometry, changes in the optical path can be visualized as interference fringes. The technique has been used to study deformations, displacements or rotations of an opaque object [21–26]. What makes this technique an interesting tool to study mass transfer processes is the fact that changes in the optical path of the light can also be due to changes in the refractive index. These refractive index changes can be caused by either temperature or concentration changes. As requisites, the system must allow the light to pass through it and changes of concentration or temperature must cause enough change in the refractive index to be detected. Holographic interferometry, as opposed to classic interferometry, presents some advantages: it is simpler and it needs only one RO cell (since the comparison is made between two images of the same cell obtained at different times); moreover, crystals of high optical quality in the

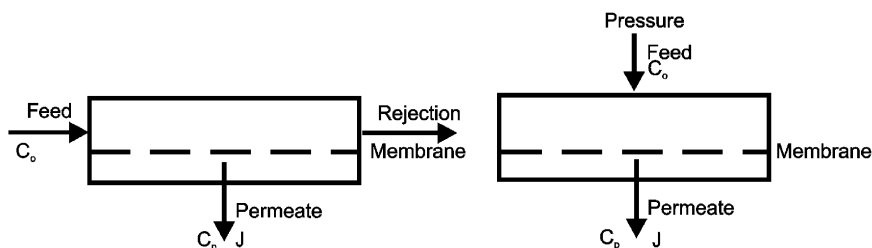


Fig. 1. Scheme of a cross-flow and a batch reverse osmosis module.

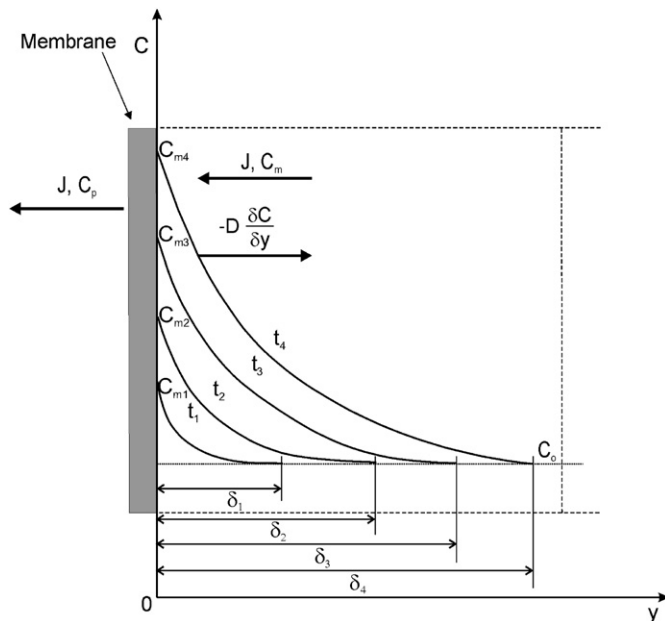


Fig. 2. Schematic concentration profiles at different times in an unstirred batch module during the appearance of the polarized layer.

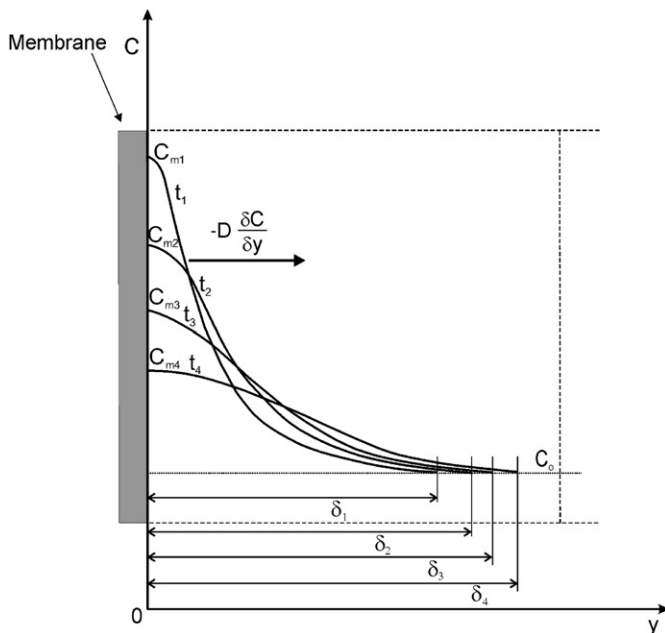


Fig. 3. Schematic concentration profiles at different times in an unstirred batch module during the disappearance of the polarized layer.

windows of the RO module are not necessary, since the small heterogeneities that could be present in them do not disturb the measurements.

2. Experimental set-up

To study by means of holographic interferometry the disappearance of the polarization layer as a consequence of the diffusion mechanism, it is necessary to visualize the zone next to the membrane. That implies combining the holographic interferometry and the RO systems, with the

RO module as common element. Moreover, the experimental set-up must satisfy some conditions:

- The RO module must allow the laser beam pass through it.
- The region of solution closest to the membrane surface must be visible.
- Interference fringes should only appear as a consequence of concentration changes.

2.1. Holographic interferometry system

The holographic interferometry system can be observed in Fig. 4. The beam coming from the laser (an He-Ne laser, Spectra Physics model 127, 35 mV, which emits coherent light at 632.8 nm) (La) is divided in two by means of a variable attenuator/beam splitter (Newport Corporation model 930-63) (BS), which ensures that both beams have equal period and wavelength. One of them, after modifying its direction in a mirror (M2), expands with a lens (L2), illuminates the object (the RO module) and the light that this object spreads (object beam) impinges on a photosensitive plate where the information of the beam is recorded (hi-res holographic plate) (HP). The other beam (reference beam) expands (L1) and, after being reflected by the other mirror (M3), it impinges on the photosensitive plate. The digital shutter system (DSS) (Newport Corporation model 845 HP) is used to fix the time of exhibition of the holographic plate to the laser beam. A film holder/processor (FHP) (Newport Corporation model 550) is used to chemically process the holographic plate and allows the plate to be fixed in place during all the experiment to avoid plate shifting. The image from the holographic plate is focused by means of another lens (L3) on a lens-less video camera (VC) (Sony CCD, mod. AVC-D7CE). The video camera is connected to a computer (PC) where images are recorded. The whole optical system is placed on an optical table (Newport Corporation M-RS-48-8) provided with three vibration isolated legs (Newport Corporation XLB2A-28T). The whole experimental apparatus is placed in a room at constant temperature, 25 ± 0.2 °C.

2.2. Reverse osmosis module

A specially designed RO module (dead-end cell) was designed in order to adapt it to the requirements of the holographic interferometry technique (Fig. 5).

To ensure physical stability, the RO module was made of stainless steel. The module was provided with two transparent glass windows thus allowing the membrane surface to be visualized. The glass was thick enough to avoid deformations caused by the pressure. Moreover, the glue used in the windows did not become deformed at the working pressure. To ensure that the region of solution closest to the membrane surface is visible, a special design of the RO module has been used, with no watertight joint on the

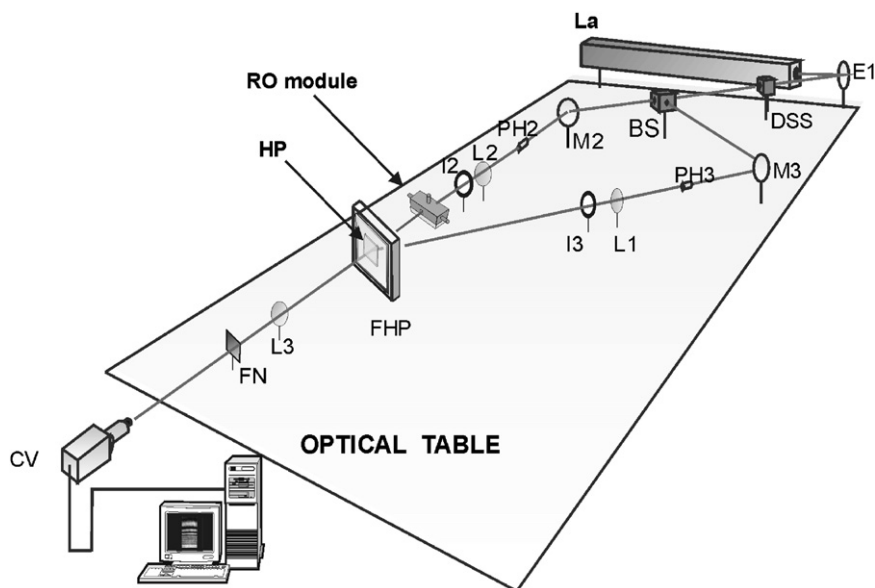


Fig. 4. Holographic interferometry system.

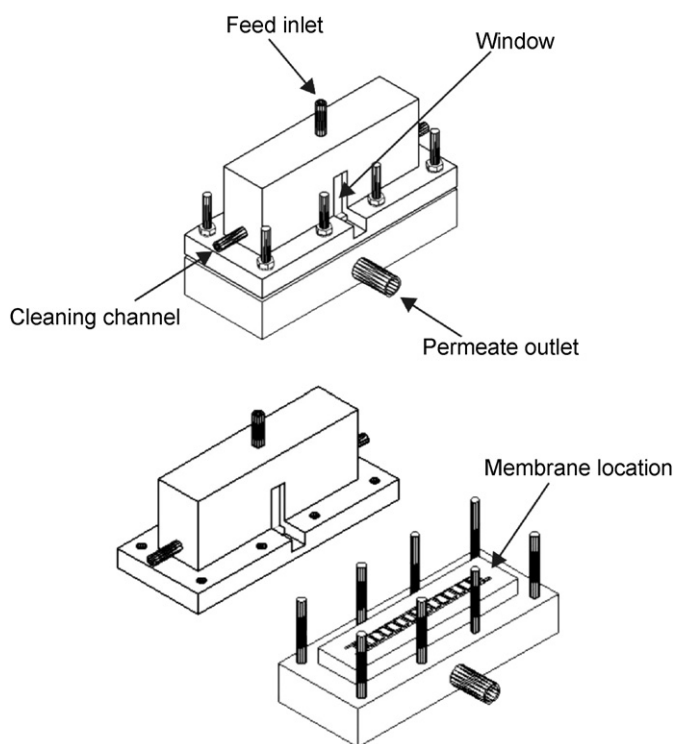


Fig. 5. RO module employed.

membrane to seal the module. A detailed description of the RO module used can be found in a previous paper [27].

The active membrane dimensions are 10×1 cm with a 10 cm^2 effective area, a size chosen to satisfy the interferometric requirements.

2.3. Reverse osmosis system

The RO set-up is shown in Fig. 6. It consists of several parts, where the RO module (6) is the main element. The

RO module was horizontally placed on the optical table and was the common element between both the RO and the holographic interferometry set-ups.

The module is connected to two vessels (8), one of them contains the solution to filter and the other, water for cleaning the membrane. The entrance of liquids to the system is regulated by means of a three-way valve.

The pressure necessary to run the process was supplied by means of pressurized nitrogen (1). In order to avoid the appearance of bubbles in the solution, the gas and the solution were separated by a damper (Hidracar S.A, V007A05E1-AI) (5). This damper, that is normally used to avoid the bursts of pressure produced by a piston pump, contains in its interior a membrane of elastic material that separates the gas from the solution and is able to resist high pressures (up to 60 bar).

Permeate coming out of the module, passes through a conductivity cell (10) connected to a conductivity (12) that continuously sends data to a computer (13). In this way, the permeate concentration, and therefore the membrane retention, can be calculated at every moment. The permeate solution is placed in a container on a balance (11) connected to the computer. The weight is registered every few seconds and allows the permeate volume curve to be obtained.

Both the pipes and the connection pieces between elements of the system are made of stainless steel, since they must be resistant to the pressure.

3. Materials and method

3.1. Materials

The membrane used was a thin film membrane, TFM-50 from Hydro Water S. L. Suitable pieces for the size of the cell used were cut from the whole membrane. Each piece of

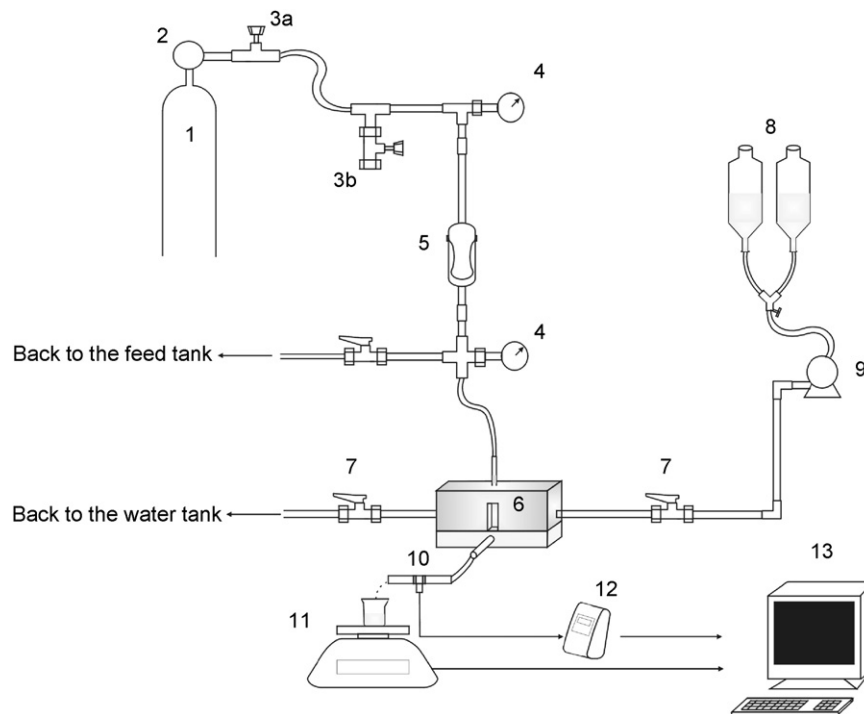


Fig. 6. Reverse osmosis system: (1) nitrogen cylinder; (2) pressure-control valve; (3a and b) precision regulation valves; (4) pressure gauges; (5) damper, (6) RO module; (7) inlet and outlet valves; (8) feed and water tanks; (9) pump; (10) conductivity probe; (11) permeate collector vessel and balance; (12) conductimeter; (13) computer.

membrane was used for several experiments, so after each experiment the cell was washed with distilled water until the salt was completely removed from the membrane surface. The membrane was considered to be clean when the permeate flux of water was recovered.

The experiments were carried out using solutions of KNO_3 (Panreac). Different feed concentrations (C_0) ranging from 1 to 7 kg/m^3 were used in order to study the effect of feed concentration on the appearance and disappearance of the polarization layer.

3.2. Experimental methodology to obtain interferograms

The membrane was placed in the bottom part of the module and the upper part was put into place. Then, the module was mounted and placed on the optical table. Pure water was pumped through the RO system for 30 or 40 min, until the permeate flux became constant. Measurement of the water flux was made in a continuous way by using a balance connected to a computer.

Once the water flux was checked, the module was filled with the solution and correctly aligned with the optical set-up. Then a hologram of the cell was recorded in the holographic plate in order to obtain the reference state for the interferometric study. To do this, the room was kept in darkness and the path of the laser beam was blocked by means of the DSS. The holographic plate was placed in the film holder/processor and the DSS was opened, impinging the object beam (after passing through the ultrafiltration module) and the reference beam on

holographic plate. With the room still in darkness, the plate was chemically processed in the same film holder/processor (the holographic plate was not moved from its original position) to avoid modifications due to plate shifting. The holographic plate processed was the hologram. After that, the laser beam was again allowed to pass through the holographic plate. Later, when pressure (all the experiments were run at a constant pressure of 600 kPa) was applied to the system ($t = 0$) and the laboratory lights switched on, the RO process could be followed (real-time holographic interferometry) as it took place as a succession of interferometric images (interferograms): during the RO process, potassium nitrate molecules reached the membrane surface due to the pressure gradient and remained there because the membrane did not allow them to pass through. Thus, the salt concentration increased above the membrane surface and a concentration profile appeared. This concentration profile resulted in a refractive index gradient. The comparison between the reference state recorded on the hologram and the evolution of the RO process caused the appearance of the interference fringes (interferogram). Each interference fringe corresponded to a certain concentration change in the solution. The relationship between concentration and refraction index was measured at $\lambda = 589 \text{ nm}$ using a refractometer (Leica, AR600) at 25°C (Table 1), which was the operation temperature. Each interferometric fringe represented a change in the refractive index. Recording of the interferograms was carried out continuously by a lens-less video camera.

Table 1
Refractive index and diffusion coefficient of aqueous solutions of KNO₃

Concentration (kg/m ³)	Refractive index ^a	$D \times 10^9$ (m ² /s) ^b
1	1.33302	1.81
2	1.33311	1.80
3.5	1.33325	1.79
5	1.33339	1.78
7	1.33358	1.77

^aExperimentally measured.

^bFrom bibliography [22].

After ceasing the pressure, the recording of the experiment continued for some time in order to visualize the disappearance of the polarized layer.

3.3. Methodology to quantitatively obtain concentration profiles

The interferograms were continuously recorded using a video camera connected to a PC. The video-capture software used allowed 24 images each second to be captured, so the quantity of interferograms registered during each experiment was very high.

In each interferogram, a series of interference fringes appeared superimposed on the image of the module whenever the following condition is satisfied:

$$\Delta(n \cdot d) = \frac{(2k + 1)\lambda}{2}, \quad (1)$$

where $\Delta(n \cdot d)$ is the change in the optical path between two fringes, k is the interference order, λ is the wavelength of the light used (632.8 nm) and d is the thickness of the liquid that the light passes through. In our case, as d remains constant ($d = 1$ cm), the formation of a new fringe implies a change in refractive index equal to Δn which corresponds to a change in potassium nitrate concentration equal to ΔC .

The methodology to quantitatively obtain concentration profiles can be summarized as follows (this process is carried out from the interferograms recorded on the video):

- (1) To take note of the original position of the membrane surface before each experiment. We attribute $y = 0$ to this position.
- (2) To follow the evolution of the recorded experiment, attributing an order number to each fringe that appears: the first fringe, 1; the second, 2 and so on.
- (3) To freeze one image from the recorded video, corresponding to a certain time after the beginning of the experiment.
- (4) To locate visually, on this image the position of the maximum darkness related to each fringe with respect to the original position of the membrane surface.
- (5) To determine Δn between two adjacent fringes from Eq. (1). In our case, as d is constant ($d = 1$ cm), $\Delta n = 6.328 \times 10^{-5}$.

- (6) To calculate the corresponding refractive index for each fringe, using the following expression:

$$n = n_o + (\text{order number}) \times \Delta n, \quad (2)$$

where n_o is the refractive index of the initial feed solution whose concentration is C_o . That is to say, a refractive index is attributed to each fringe related to each order number. The first fringe implies one change in the refractive index with respect to that corresponding to the feed solution, the second fringe two changes, and so on.

- (7) To calculate the concentration corresponding to each refractive index (n) at the position of the fringe (Table 1).
- (8) To plot concentration vs. distance from the membrane.

The process is graphically summarized in Fig. 7. It can be seen in the figure that the distance of each fringe from the membrane surface is obtained from one chosen interferogram (a). Diagrams (b) and (c) show pairs of data for each fringe: refractive index or concentrations with distance.

4. Results and discussion

4.1. Visualization of the polarized layer

In order to visualize the polarized layer, several RO experiments at different potassium nitrate concentrations, varying between 1 and 7 kg/m³, were carried out in an unstirred batch module. By means of holographic interferometry, it has been possible to follow in real time the appearance, evolution and disappearance of the concentration polarization layer during dead-end RO experiments. In all the experiments, transmembrane pressure was kept constant at 600 kPa.

Experimental conditions are shown in Table 2, where J_w is the volumetric permeate flux with pure water before the beginning of the RO experiment and R_m is the membrane hydraulic resistance to the flux with pure water, which is calculated with Eq. (3):

$$J_w = \frac{\Delta P}{R_m}. \quad (3)$$

The area observed indicates the true dimensions of the rectangular zone visualized by means of the optical system and depends on the magnification needed in each case, which is obtained by using a lens to focus the image on the camera. Reproducibility of the behavior observed was confirmed by repeating the RO runs in the same conditions (solute and initial feed concentration).

A few minutes after the RO process started some interferometric fringes near the membrane surface appeared. The amount of fringes continued increasing throughout the process, thus indicating that the concentration at the membrane surface (C_m) was increasing, as well

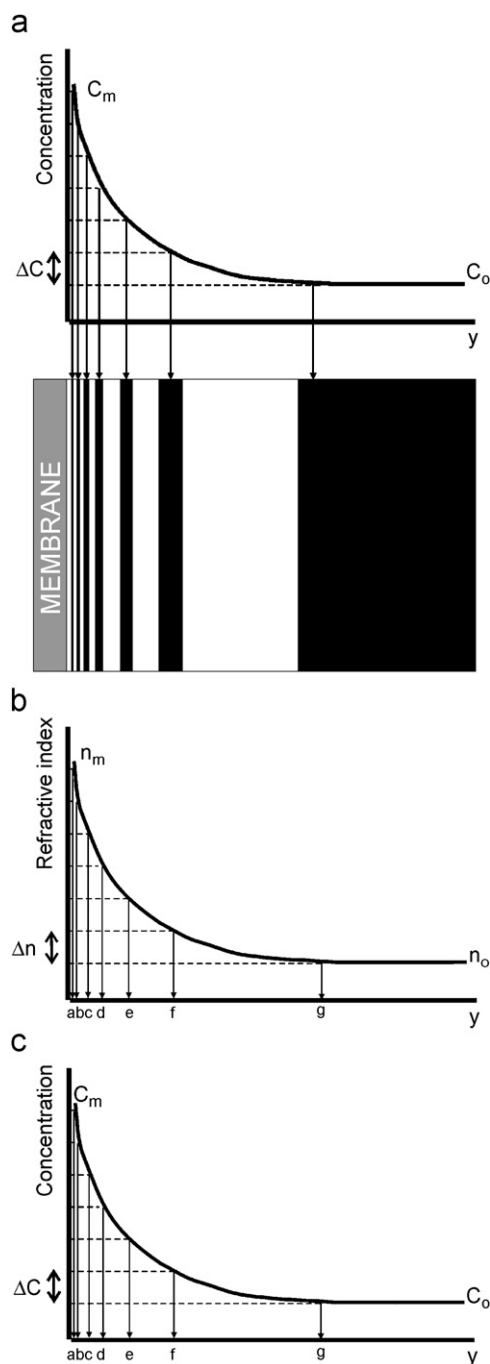


Fig. 7. Equivalence between the interferograms and the concentration profiles.

as the thickness of the boundary layer (δ). The rate of appearance of new interference fringes was high during the first few minutes of the experiment, but later it decreased. Most of the polarization layer was developed during, approximately, the first hour of the process.

Once the pressure ceased and the RO process ended, the fringe pattern changed. The convective force disappeared and only the diffusive process remained. The interference fringes became wider and more separated, slowly disappearing as a consequence of this diffusive process. Interferograms in Figs. 8 and 9 correspond to 1, 2, 15,

30, 60 and 90 min after the end of the RO process, for two experiments with different potassium nitrate concentration ($C_o = 1$ and 7 kg/m^3). As can be observed in both figures, the number of fringes decreased with time and the remaining ones were wider and more separated between themselves, as well as from the membrane. This behavior indicates that the concentration at the membrane surface (C_m) decreases and the thickness of the boundary layer increases with time. Therefore, the slope of the concentration profiles becomes smoother with time, until the concentration gradient completely disappears. The disappearance of the polarization layer is a very slow process (for instance, 60 min after the end of the RO process some interference fringes were still visible). This evolution of the interference fringes is a consequence of the diffusive solute flow from the membrane surface to the bulk solution, due to the concentration gradient between them generated during the RO process. This behavior proves that concentration polarization in RO processes is a reversible A Video (<http://www.ua.es/es/servicios/si/servicios/videos-streaming/iq/holografia.html>), showing when the pressure ceased and the disappearance of the interference fringes in experiment V during 1 h and 32 min, has been prepared. In order to better perceive the changes occurring, the video reproduces the images at 25 times the speed of the process (as a consequence, the Video is 3 min and 40 s long).

4.2. Concentration profiles

Interference fringes which appeared in the interferograms were the result of a refractive index gradient in the vicinity of the membrane due to a concentration gradient. Because a relationship exists between the refractive index and concentration (Table 1), it was possible, using the methodology previously explained, to obtain the concentration profile from the interference fringes. Once the pressure ceased, the concentration profile near the membrane surface was disappearing as a consequence of solute returning to the bulk solution due to the diffusion phenomenon.

Table 3 shows the number of interference fringes, the distance (y) to the membrane for each fringe and its concentration (C) corresponding to this disappearance of fringes. The evolution of the concentration profiles of these experiments can be observed more clearly in Fig. 10. It can be observed that the slope of the concentration profile becomes smoother with time, as a consequence of the decrease in the solution concentration at the membrane surface and the increase of the thickness of the boundary layer.

4.3. Simulation of the disappearance process

Theoretical models describing dead-end RO processes usually combine both the unsteady-state mass balance in the polarization layer and the osmotic pressure model. In the mass balance, a convection–diffusion mechanism

Table 2
Experimental conditions

Exp. no	C_o (kg/m ³)	$J_w \times 10^6$ (m ³ /m ² s)	$R_m \times 10^{-11}$ (Pa s/m ²)	Area observed (mm × mm)
I	1	5.36	1.13	3.40 × 9.50
II	2	5.28	1.15	3.40 × 9.50
III	3.5	5.52	1.10	3.40 × 9.50
IV	5	5.49	1.11	3.40 × 9.50
V	7	5.65	1.08	3.40 × 9.50

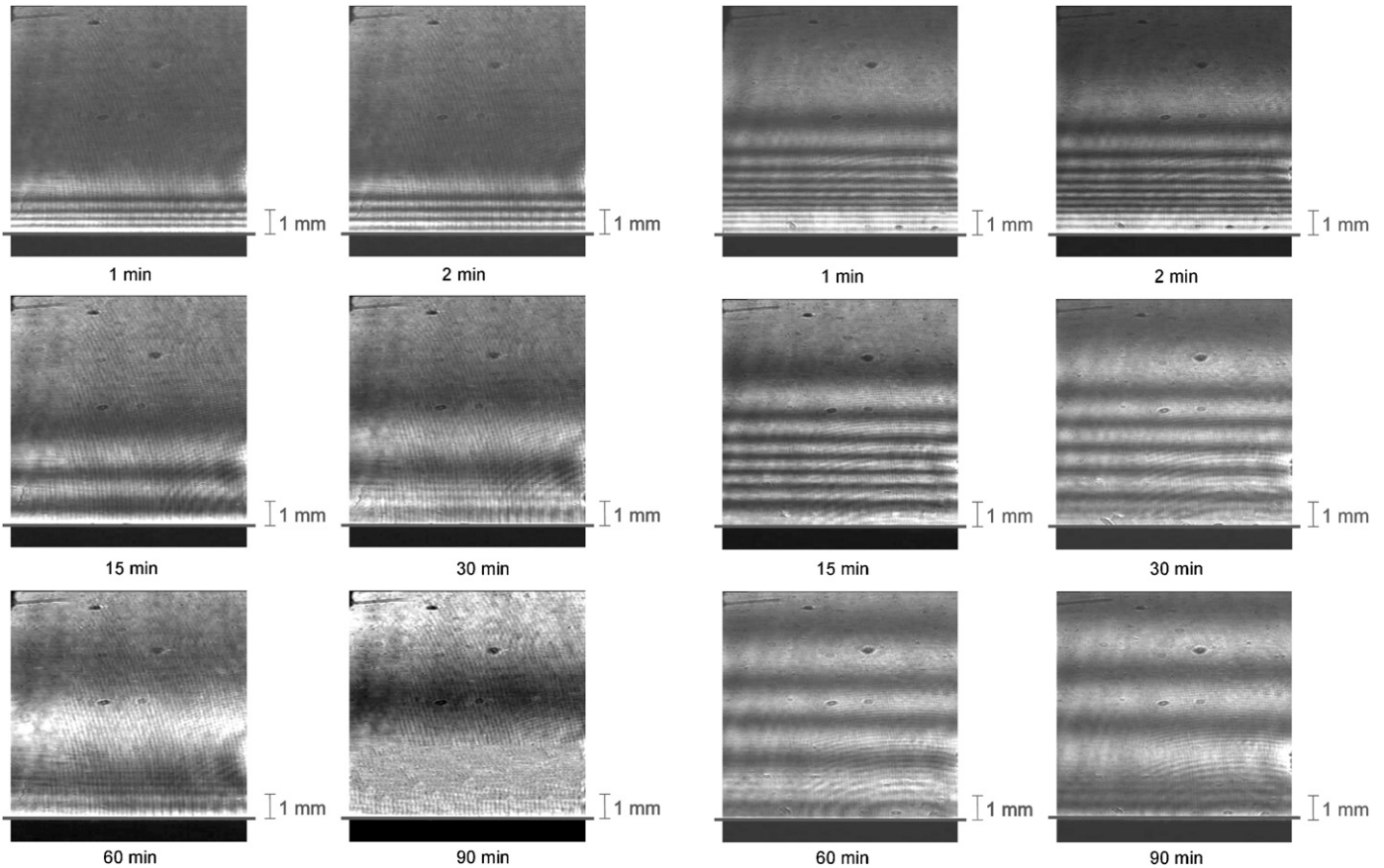


Fig. 8. Interferograms belonging to Experiment I ($C_o = 1 \text{ kg/m}^3$) at 1, 2, 15, 30, 60 and 90 min.

Fig. 9. Interferograms belonging to Experiment V ($C_o = 7 \text{ kg/m}^3$) at 1, 2, 15, 30, 60 and 90 min.

is assumed

$$\frac{\partial C}{\partial t} = J \frac{\partial C}{\partial y} + \frac{\partial}{\partial y} \left(D \frac{\partial C}{\partial y} \right). \quad (4)$$

The polarization layer disappears as a consequence of the diffusive movement of the solute accumulated during the RO process from the membrane surface to the bulk solution, caused by the concentration difference between both places. Once the convective solute flow due to the pressure applied ceased, diffusion was the only mass transfer mechanism involved. So the constitutive equation in this case is:

$$\frac{\partial C}{\partial t} = \frac{\partial}{\partial y} \left(D \frac{\partial C}{\partial y} \right). \quad (5)$$

Assuming the diffusion coefficient is a constant, Eq. (5) becomes

$$\frac{\partial C}{\partial t} = D \frac{\partial^2 C}{\partial y^2}, \quad (6)$$

which is Fick's second law.

In order to calculate concentration profiles during the disappearance of the polarized layer, Eq. (6) was numerically solved, using the first concentration profile obtained by holographic interferometry (60 s after the RO process finished) as the initial condition. The diffusion coefficient (Table 1) was obtained from bibliography [28]. A constant value of the diffusion coefficient (according to data in Table 1) was used for each concentration profiles studied. Experimental and calculated concentration profiles appear

Table 3
KNO₃ concentration profiles during the disappearance of the polarized layer

Interferogram Fringe order no.	y (mm)						C (kg/m ³)
	at 1 min	at 2 min	at 15 min	at 30 min	at 60 min	at 90 min	
Experiment I: C ₀ = 1 kg/m ³							
1	3.99	2.71	4.11	5.40	6.242	4.897	1.68
2	1.44	1.53	2.10	2.28	1.675		2.35
3	0.94	1.01	0.74	0.24			3.03
4	0.61	0.61					3.71
5	0.32	0.18					4.38
Experiment II: C ₀ = 2 kg/m ³							
1	4.47	3.36	4.51	6.80	9.64	7.76	2.68
2	2.07	2.07	2.82	3.51	4.25	2.78	3.35
3	1.48	1.54	1.88	1.92	0.58		4.03
4	1.15	1.18	0.92	0.17			4.71
5	0.85	0.85					5.38
6	0.66	0.56					6.06
7	0.38	0.24					6.74
Experiment III: C ₀ = 3.5 kg/m ³							
1				8.97	8.65	8.51	4.18
2	5.68	6.05	4.71	5.47	5.43	4.98	4.85
3	2.87	3.12	3.40	3.74	3.22	1.96	5.53
4	2.13	2.30	2.52	2.54	0.50		6.21
5	1.71	1.80	1.82	1.34			6.88
6	1.36	1.45	1.13				7.56
7	1.08	1.13					8.24
8	0.87	0.87					8.91
9	0.65	0.58					9.59
10	0.40	0.35					10.27
11	0.12						10.97
Experiment IV: C ₀ = 5 kg/m ³							
1			8.37	8.12	8.77	6.95	5.68
2	5.70	5.63	4.88	5.13	5.86	4.29	6.35
3	3.55	3.51	3.62	3.81	3.97	0.86	7.03
4	2.58	2.67	2.83	2.74	2.01		7.71
5	2.06	2.13	2.12	1.69			8.38
6	1.69	1.72	1.47	0.37			9.06
7	1.38	1.41	0.71				9.74
8	1.12	1.12					10.41
9	0.89	0.84					11.09
10	0.66	0.59					11.77
11	0.43	0.23					12.44
12	0.14						13.12
Experiment V: C ₀ = 7 kg/m ³							
1	8.96	8.33	6.37	8.33	8.01	9.10	7.68
2	4.63	4.38	4.59	5.59	5.66	6.14	8.35
3	3.40	3.30	3.63	4.26	4.05	3.81	9.03
4	2.70	2.60	2.91	3.28	2.47	1.10	9.71
5	2.19	2.16	2.24	2.37	0.49		10.38
6	1.84	1.81	1.65	1.26			11.06
7	1.51	1.49	0.86	0.65			11.74
8	1.21	1.19					12.41
9	1.02	0.95					13.09
10	0.74	0.63					13.77
11	0.53	0.33					14.44
12	0.25						15.12

in Fig. 10 and show a good agreement thus indicating the diffusion theory can adequately describe the disappearance of the polarization layer near the membrane. As can be observed, the slope of the concentration pro-

file becomes smoother with time and therefore, the concentration change is less. This small change in concentration explains the intersection of the profiles at different times.

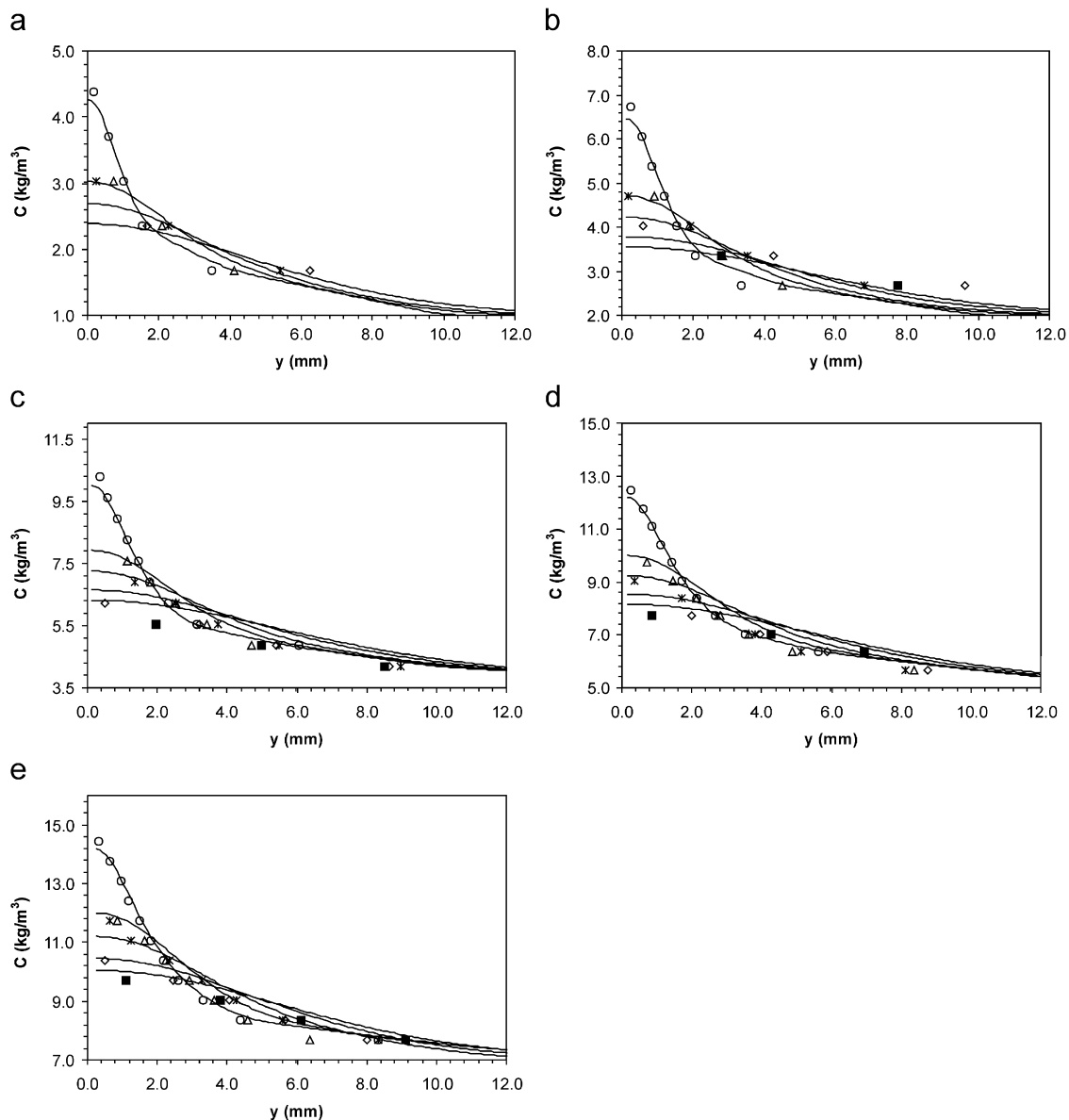


Fig. 10. Experimental and calculated concentration profiles at different times (○: 2 min, △: 15 min, *: 30 min, ◇: 60 min, ■: 90 min, —: model calculation). (a) Experiment I: $C_0 = 1 \text{ kg/m}^3$; (b) Experiment II: $C_0 = 2 \text{ kg/m}^3$; (c); Experiment III: $C_0 = 3.5 \text{ kg/m}^3$ (d); Experiment IV: $C_0 = 5 \text{ kg/m}^3$; (e) Experiment V: $C_0 = 7 \text{ kg/m}^3$.

Main differences between experimental and calculated values in Fig. 10 correspond to the region closest to the membrane. Possibly, these differences are due, on one hand, to the experimental error measuring the interference fringes near the membrane and, on the other hand, to the fact that the numerical simulation is more difficult when the slope of the concentration profiles is steeper as it occurs in the proximity of the membrane.

5. Conclusions

Holographic interferometry is a useful non-invasive technique that allows studying the effect of diffusion on the disappearance of the concentration polarization layer during RO processes. It has been used to follow, as

interference fringes, the evolution with time and the disappearance of the polarization layer in dead-end RO of aqueous solutions of KNO_3 .

Concentration profiles, after the pressure ceased, have been experimentally obtained and it has been possible to study the disappearance of the polarization concentration layer, concluding that the polarization phenomenon is a reversible process. A mathematical model, based on a diffusive mechanism, has been proposed. Agreement between experimental and calculated concentration profiles validates the model.

Acknowledgments

This research was sponsored by the Plan Nacional de I+D+I BQU2000-0456 (Ministerio de Educación y Cultura)

and by the Ajuda per a Grups de I+D+I de la Conselleria d'Empresa, Universitat i Ciència (Generalitat Valenciana).

References

- [1] Ruiz-Bevia F, Celdran-Mallol A, Santos-Garcia C, Fernandez-Sempere J. Liquid diffusion measurement by holographic interferometry. *Can J Chem Eng* 1985;63:765–71.
- [2] Ruiz-Bevia F, Celdran-Mallol A, Santos-Garcia C, Fernandez-Sempere J. Holographic interferometric study of free-diffusion: a new mathematical treatment. *Appl Opt* 1985;24(10):1481–4.
- [3] Ruiz-Bevia F, Fernandez-Sempere J, Boluda-Botella N. Variation of phosphoric acid diffusion coefficient with concentration. *AIChE J* 1995;41:185–9.
- [4] Fernandez-Sempere J, Ruiz-Bevia F, Colom-Valiente J, Más-Pérez F. Determination of diffusion coefficients of glycols. *J Chem Eng Data* 1996;41:47–8.
- [5] Ruiz-Bevia F, Fernandez-Sempere J, Colom-Valiente J. Diffusivity measurement in calcium alginate gel by holographic interferometry. *AIChE J* 1989;35(11):1895–8.
- [6] Gustafsson NO, Westrin B, Axelsson A, Zacchi G. Measurement of diffusion coefficients in gel using holographic interferometry. *Biotechnol Prog* 1993;9:436–41.
- [7] Roger P, Mattisson Ch, Axelsson A, Zach G. Use of holographic laser interferometry to study the diffusion of polymers in gel. *Biotechnol Bioeng* 2000;69(6):654–63.
- [8] Liu M, Williams FA. Concentration polarization in an unstirred batch cell: measurements and comparison with theory. *Int J Heat Mass Transfer* 1970;13:1441–57.
- [9] Goldsmith H, Lolachi H. Test cell for measuring the concentration polarization boundary layer in a reverse osmosis system. *US Office Saline Water, Res Develop Prog Rep no. 527*, 1970.
- [10] Hendricks TJ, Williams FA. Diffusion-layer structure in reverse osmosis channel flow. *Desalination* 1971;9:155–80.
- [11] Williams FA; Hendricks TJ, Macquin JF. Observations on buoyant convection in reverse osmosis. *Ind Eng Fundam* 1972;11(2):276–9.
- [12] Johnson AR. Experimental investigation of polarization effects in reverse osmosis. *AIChE J* 1974;20(5):966–74.
- [13] Mahlab D, Yosef NB, Belfort G. Concentration polarization profile for dissolved species in unstirred batch hyperfiltration (reverse osmosis)—II transient case. *Desalination* 1978;24:297–303.
- [14] Clifton M, Sanchez V. Holographic interferometry applied to the measurement of boundary layers in electro dialysis and ultrafiltration. *SPIE*, 211. *Opt Photonics Appl Med* 1979, 111–5.
- [15] Vilker VL, Colton CK, Smith KA, Green DL. Concentration polarization in protein U.F. Part I: an optical shadowgraph technique for measuring concentration profiles near a solution–membrane interface. *AIChE J* 1981;27(4):632–7.
- [16] Vilker VL, Colton CK, Smith KA, Green DL. Concentration polarization in protein U.F. Part II: theoretical and experimental study of albumin ultrafiltered in an unstirred cell. *AIChE J* 1981;27(4):637–45.
- [17] Fernández Torres MJ, Ruiz-Beviá F, Fernández-Sempere J, López-Leiva M. Visualization of the UF polarized layer by holographic interferometry. *AIChE J* 1998;44:1765–76.
- [18] Fernández-Sempere J, Ruiz-Beviá F, Salcedo-Díaz R. Measurements by holographic interferometry of concentration profiles in dead-end ultrafiltration of polyethylene glycol solutions. *J Membr Sci* 2004;229:187–97.
- [19] Fernández-Sempere J, Ruiz-Beviá F, Salcedo-Díaz R, García-Algado P. Measurement of concentration profiles by holographic interferometry and modelling in unstirred batch reverse osmosis. *Ing Eng Chem Res* 2006;45:7219–31.
- [20] Fernández-Sempere J, Ruiz-Beviá F, Salcedo-Díaz R, García-Algado P. Buoyancy effects in dead-end reverse osmosis. Visualization by holographic interferometry. *Ind Eng Chem Res* 2007;46:1794–802.
- [21] Brooks RE, Heflinger LO, Wuerker RF. Interferometry with a holographically reconstructed comparison beam. *Appl Phys Lett* 1965;7:248–9.
- [22] Heflinger LO, Wuerker RF, Brooks RE. Holographic interferometry. *J Appl Phys* 1966;37:642–9.
- [23] Stetson KA. Fringe interpretation for hologram interferometry of rigid-body motions and homogeneous deformations. *J Opt Soc Am* 1974;64:1–10.
- [24] De Nicola S, Ferraro P, Finzio A, Pierattini G. Analysis of rigid rotations in holographic interferometry for simple flexural loading tests. *Opt Lasers Eng* 1997;27:369–78.
- [25] Frejlich J, Garcia P M. Advances in real-time holographic interferometry for the measurement of vibrations and deformations. *Opt Lasers Eng* 2000;32:515–27.
- [26] Schumann W. Deformation measurement by holographic interferometry. Analysis on curved surfaces. General aspects. *Opt Lasers Eng* 2002;37:1–13.
- [27] Fernández-Sempere J, Ruiz-Beviá F, Salcedo-Díaz R, García-Algado P. Estudio de la capa de polarización durante el proceso de ósmosis inversa. Equipo experimental para visualizar la formación de la capa. *Ingeniería Química* 2006;438:147–54.
- [28] Albright JG, Vinod D. Measurement of mutual-diffusion coefficients for the system potassium nitrate-water at 25 °C. *J Solution Chem* 1991;20(6):633–42.